https://doi.org/10.17221/25/2020-SWR

Estimation of annual mean rainfall erosivity based on hourly rainfall data in a tropical region

Ming-Hsi Lee, I-Ping Hsu*

Department of Soil and Water Conservation, National Pingtung University of Science and Technology, Pingtung, Taiwan

**Corresponding author: mhlee@mail.npust.edu.tw*

Citation: Lee M.H., Hsu I.P. (2021): Estimation of the annual rainfall erosivity index based on hourly rainfall data in a tropical region. Soil & Water Res., 16: 74–84.

Abstract: The annual mean rainfall erosivity (R) indicates the potential soil loss caused by the precipitation and runoff and is used to predict the soil loss from agricultural hillslopes. R is calculated from rainfall stations with continuously recording rainfall databases. However, many short-term real-time rainfall databases that also relate to the rainfall intensity are not readily available around Taiwan, with the hourly rainfall data being predominantly available. The annual mean rainfall erosivity calculated by the 10-min rainfall data accumulation converted to the 30-min rainfall data (R_{10_30}) can be estimated using the annual mean rainfall erosivity calculated by the 10-min rainfall data accumulation convert to the hourly rainfall data (R_{10_60}) that are calculated from the kinetic energy calculated by the 10-min rainfall data accumulation converted to the hourly rainfall data (E_{60j}). The maximum 60-min rainfall intensity calculated by the 10-min rainfall data accumulation converted to the hourly rainfall data (I_{60j}) has been established in rainfall stations throughout southern Taiwan. The 10-min rainfall data set consists of 15 221 storm events from 2002 to 2017 monitored by 51 rainfall stations located in the tropical regions in Taiwan. According to the results of this study, the average conversion factors of the kinetic energy (1.04), rainfall erosivity (1.47), and annual mean rainfall erosivity (1.30) could be estimated based on the 10-min rainfall data.

Keywords: climate change; soil erosion; Universal Soil Loss Equation (USLE)

Abbreviations: E_j – the kinetic energy in a rainfall event; E_{10j} – the kinetic energy calculated by the 10-min rainfall data; E_{60j} – the kinetic energy calculated by the 10-min rainfall data accumulation converted to the hourly rainfall data; e_i – the unitary kinetic energy; e_{10i} – the unitary kinetic energy calculated by the 10-min rainfall data; e_{60i} – the unitary kinetic energy calculated by the 10-min rainfall data accumulation converted to the hourly rainfall data; I_{30j} – the maximum 30-min rainfall intensity calculated by the 10-min rainfall data accumulation converted to the 30-min rainfall data; I_{60j} – the maximum 60-min rainfall intensity calculated by the 10-min rainfall data accumulation converted to the hourly rainfall data; R_j – the rainfall erosivity in a rainfall event; R_{10_30j} – the rainfall erosivity in a rainfall event calculated by the 10-min rainfall data accumulation converted to the 30-min rainfall data; R_{10_60j} – the rainfall erosivity in a rainfall event calculated by the 10-min rainfall data accumulation converted to the hourly rainfall data; R_{10_30y} – the annual rainfall erosivity calculated by the 10-min rainfall data accumulation converted to the 30-min rainfall data; R_{10_60y} – the annual rainfall erosivity calculated by the 10-min rainfall data accumulation converted to the hourly rainfall data; R – the annual mean rainfall erosivity; R_{10_30} – the annual mean rainfall erosivity calculated by the 10-min rainfall data accumulation converted to the 30-min rainfall data; R_{10_60} – the annual mean rainfall erosivity calculated by the 10-min rainfall data accumulation converted to the hourly rainfall data; j – the effective rainfall event; y – the annual rainfall event.

Wischmeier and Smith (1958) found that the product of the kinetic energy (E_j) and the maximum 30-min rainfall intensity (I_{30j}) in a rainfall event reveals a high correlation between the soil loss and rainfall intensity. Here, j showed an effective rainfall event. They defined the annual mean rainfall erosivity (R)

Supported by the Ministry of Science and Technology, Taiwan, Project No. MOST 108-2625-M-020-003-.

https://doi.org/10.17221/25/2020-SWR

as the average annual sum of the rainfall E_jI_{30j} values. The rainfall erosivity (R_j) and I_{30j} of a rainfall event are generally computed from the hyetograph data or high-resolution rainfall data (pluviograph data). Generally, a researcher must use at least 20 years of rainfall data to compute the R of a given study area when using the Universal Soil Loss Equation (USLE; Wischmeier 1959). However, such a large amount of data is not available for all regions in the world. Furthermore, the R estimation is complicated even with sufficient amount of pluviograph data available. To overcome this problem, various simplified regression equations have been proposed to estimate R by using more readily available data. Several studies have reported a significant correlation between R and E_jI_{30j} in many areas worldwide. Accordingly, the annual precipitation data have been used to obtain a simple estimation of R in numerous countries (Lawal et al. 2007; Roux et al. 2008; Angulo-Martínez & Beguería 2009; Xin et al. 2010; Bonilla & Vidal 2011; Lee & Heo 2011; Yin et al. 2015; Plangos & Udmale 2017). Detailed chart-recorded rain gauge data relative to the storm intensity are not readily available in many countries, such as China, whereas the hourly rainfall data are readily available (Yin et al. 2007a).

Due to the limited availability of the breakpoint rainfall data, many simple methods for estimating R have been developed (Ateshian 1974; Arnoldus 1977; Richardson et al. 1983; Ferro et al. 1991; Renard & Freimund 1994; Yu & Rosewell 1996; Zhang et al. 2002; Yin et al. 2015; Panagos et al. 2016). When more detailed rainfall data can be used, a more precise computation of R can be achieved. With an increase in automatic recording weather stations, fixed-interval rainfall data are increasingly available and used. Automatically recorded rainfall data in fixed time intervals may be a preferred substitute to the breakpoint data for R that are estimated through the analysis of the yearly, monthly, daily, hourly data.

Istok et al. (1986) examined 15- and 60-min interval rainfall data at three sites in a small watershed in western Oregon in the United States. All the results revealed a highly significant linear correlation between R_{15j} and R_{60j} for each site. The conversion factors between R_{15j} and R_{60j}, which are the ratios of R_{15j} and R_{60j}, ranged from 1.193 to 1.378 and were statistically different among the sites. Yin et al. (2007a) estimated R_j in central China by using 5-, 10-, 15-, 30-, and 60-min time interval rainfall data. The results indicated that the time interval was reduced from 60 to 5 min, and the average conversion factor decreased from 1.105 to 1.009 for E_j. However, the value changed from 1.668 to 1.007 and 1.730 to 1.014 for the I_{30j} and E_jI_{30j} values, respectively.

The literature describes many investigations on the correlation between R_j and the rainfall data time intervals around the world. Yin et al. (2007b) stated that because the continuous rainfall and rainfall intensity data in many parts of China were difficult to obtain, they analysed 456 rainstorm events recorded by five water and soil monitoring stations in eastern China and developed a method for estimating R with the hourly rainfall data. Yang et al. (2010) adopted the 10-min and hourly rainfall data of the drainage basin of the Zengwen Reservoir in southern Taiwan to compare the R_j that was calculated from the two types of data. Lobo and Bonilla (2015) developed a method for calculating R by using rainfall data recorded at 1–24 h intervals in Chile because rainfall data recorded at less than hourly intervals are rare worldwide. Panagos et al. (2017) argued that using annual rainfall data to calculate R could be problematic and lead to substantial biases. Therefore, they proposed estimating R with hourly rainfall data recorded by 3 625 weather stations worldwide to establish a global annual mean rainfall erosivity diagram. Fischer et al. (2018) used radar rain data to analyse rainfall in Germany. After considering the effects of the temporal scale, spatial scale, and position on the R, they proposed a modified function for low temporal resolution rainfall data. However, 30-min or under 30-min time interval rainfall data are not typically acquired because of its large volume of data or requires payment; instead, hourly rainfall data are more readily available. Moreover, the correlation between R_j and the hourly rainfall data in tropical regions has been investigated for many years. Recently, studies evaluating the R_j in tropical regions by using hourly rainfall data at rainfall stations have been considered crucial.

In Taiwan, the current practice of estimating soil erosion induced by effective rainfall involves calculating the product of the kinetic energy and maximum 30-min rainfall intensity as R_j. However, only the historical hourly or daily rainfall data are available in most areas; most areas, thus, lack the short-interval rainfall data needed to calculate the rainfall erosivity as well as the long-term (yearly) radar rain data. The insufficient precision in rainfall data has resulted in calculation difficulties. Therefore, this study developed a method of estimating the annual mean rainfall erosivity by using readily available hourly

https://doi.org/10.17221/25/2020-SWR

rainfall data. Most rainfall stations in Taiwan have begun recording 10-min rainfall data to measure the kinetic energy of an effective rainfall event, the rainfall erosivity of a rainfall event, and the annual mean rainfall erosivity for a more precise estimation. The results of this study may serve as a reference for competent authorities to estimate the annual mean rainfall erosivity in Taiwan's tropical region by using hourly rainfall data when short-interval rainfall data are unavailable.

MATERIAL AND METHODS

This study collected the 10-min rainfall data recorded from 2002 to 2017 by fifty-one rainfall stations distributed throughout Kaohsiung City and Pingtung County, which are both situated in the tropical region of Taiwan. This study applied the definition of a single effective rainfall event proposed by Wischmeier and Smith (1958) to identify effective rainfall events within the area. The kinetic energy (E_{10j} and E_{60j}) of each effective rainfall event, maximum rainfall intensity (I_{30j} and I_{60j}), and rainfall erosivity of a rainfall event (R_{10_30j} and R_{10_60j}) were calculated by the 10-min rainfall data and were subsequently used to determine the annual mean rainfall erosivity (R_{10_30} and R_{10_60}). Here, 10_30 showed the 10-min rainfall data accumulation convert to the 30-min rainfall data and 10_60 showed the 10-min rainfall data accumulation convert to the hourly rainfall data. This study used the 10-min rainfall data, which were chosen to more accurately estimate the kinetic energy (E_{10j}) of an effective rainfall event, and the 30-min rainfall data were obtained by accumulating the 10-min data to calculate the maximum rainfall intensity (I_{30j}), a parameter required by all contemporary rainfall erosivity calculation methods. In addition, the 60-min rainfall data were obtained by accumulating the 10-min data to estimate R_{30} when accurate historical rainfall data or short-interval rainfall data were lacking. In particular, this study used the 10-min rainfall data to establish conversion coefficients for E_{10j} and E_{60j}, I_{30j} and I_{60j}, R_{10_30j} and R_{10_60j}, and R_{10_30} and R_{10_60}. Finally, a regression analysis was performed to find the conversion coefficients for the kinetic energy, maximum rainfall intensity, and annual mean rainfall erosivity from the rainfall data at different time intervals.

Southern Taiwan Region. Two tropical regions with an area of 2 961 km^2 (Kaohsiung City) and 2 784 km^2 (Pingtung County) surrounded by fifty-one Central Weather Bureau rainfall stations in southern Taiwan were selected for this study (Figure 1). Kaohsiung City and Pingtung County are both located within the south of the Tropic of Cancer in southern Taiwan. They are located in a tropical monsoon climate; the winters are dry and the summers are rainy. The average annual temperatures in Kaohsiung City and Pingtung County were 25.1 and 25.2 °C, respectively, with the lowest temperatures occurring in January (the average monthly temperatures were 19.3 and 20.7 °C, respectively), and with the highest temperatures occurring in July (the average monthly temperatures were 29.2 and 28.4 °C, respectively). In winter (December–February), the weather is affected by the continental air mass and the northeast monsoon, but is relatively dry due to the Central Mountain Range in Taiwan blocking the systems, with an average monthly rainfall of 18 mm and 23 mm, respectively. In the summer (June to August), the regions receive most rainfall (the average monthly rainfall in Kaohsiung City and Pingtung County are 381 and 412 mm, respectively), mainly

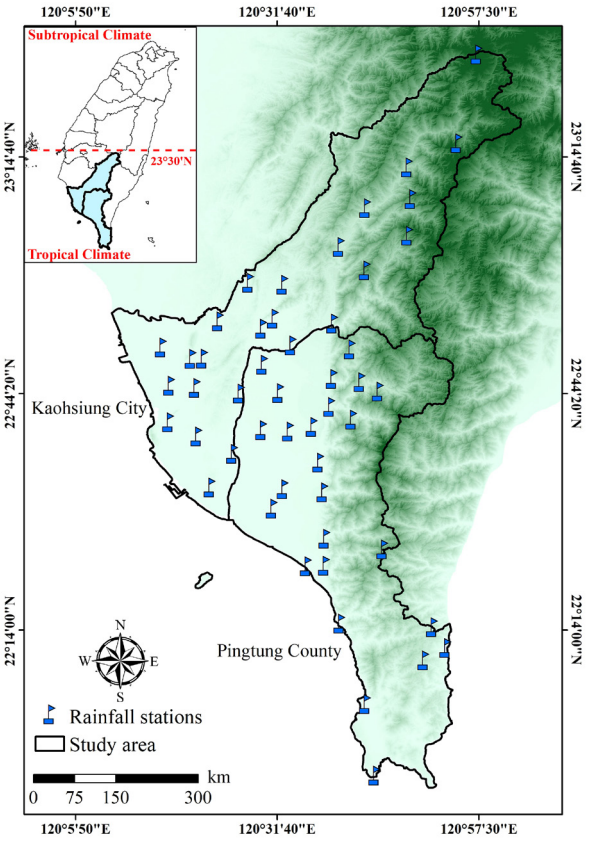

Figure 1. Map of the fifty-one rainfall stations in the study area

https://doi.org/10.17221/25/2020-SWR

due to the influence of the plum rain, maritime air mass and southwest monsoons, which are vulnerable to thunderstorms and typhoons. Extreme rainfall events occur frequently in these regions during the summer, which trigger severe changes in the watershed environment and cause major sediment disasters. An example is Typhoon Morakot in 2009, where 665 people were killed, 34 people went missing, and approximately 4.4 billion USD was caused in damage as a result. When it struck Taiwan over August 5–10, the maximum accumulative rainfall in Kaohsiung City and Pingtung County reached 2 517 and 2 686 mm (the annual mean rainfall of Kaohsiung City and Pingtung County are 1 885 mm and 2 022 mm), respectively.

Material. The product of the kinetic energy and maximum 30-min rainfall intensity is the primary parameter for the estimation of the soil loss induced by an effective rainfall event. For areas with only hourly or daily rainfall data available, estimating the rainfall erosivity can be difficult. In Taiwan, although most rainfall stations have begun recording 10-min rainfall data, historical records are predominately comprised of hourly data. Therefore, this study collected 10-min rainfall data from the fifty-one rainfall stations within the research area, which recorded 15 221 effective rainfall events between 2002 and 2017. Specifically, the 10-min rainfall and 10-min accumulative rainfall data were used to estimate the kinetic energy (E_{10j} and E_{60j}) of an effective rainfall event, the maximum rainfall intensity (I_{30j} and I_{60j}), and the rainfall erosivity in a rainfall event (R_{10_30j} and R_{10_60j}). These parameters were subsequently employed to determine the conversion coefficients for the kinetic energy, maximum rainfall intensity, and annual mean rainfall erosivity when the rainfall data with different time intervals were used. The conversion method is detailed in the following section.

Establishing the relationship between R_{10_30} and R_{10_60} based on the 10-min rainfall data. The rainfall erosivity in a rainfall event calculated by the 10-min rainfall data accumulation converted to the 30-min rainfall data (R_{10_30j}) describes the erosive impact of the rainfall and runoff on the detachment and entrainment of the soil, which can be expressed as Equation (1)

$$R_{10\_30j} = E_{10j} \times I_{30j} = \sum_{i=1}^{T_i} \left(e_{10i} P_{ji}\right) \times I_{30j} \quad (1)$$

where:

E_{10j} – the kinetic energy calculated by the 10-min rainfall data (MJ/ha),

I_{30j} – the maximum 30-min rainfall intensity calculated by the e10-min rainfall data accumulation converted to the 30-min rainfall data (mm/h),

e_{10i} – the unitary kinetic energy calculated by the 10-min rainfall data (MJ/mm·ha),

P_{ji} – the rainfall amount (mm),

T_i – the total rainfall duration,

i, j – the number of rainfall data instances and the number of rainfall events, respectively.

By adding the R_{10_30j} of all rainfall events in one year, the annual rainfall erosivity calculated by the 10-min rainfall data accumulation converted to the 30-min rainfall data (R_{10_30y}) can be derived as follows:

$$R_{10\_30y} = \sum_{j=1}^{Y} R_{10\_30j} \quad (2)$$

where:

Y – the number of rainfall events in the year.

In addition, the unitary kinetic energy (e_i) is deduced from the relationship between the raindrop diameter and the rainfall intensity, as follows (Laws & Parsons 1943):

$$e_i = \begin{cases} 0.119 + 0.0876 \log I_i & \text{for } I_i < 76 \text{ mm/h} \\ 0.283 & \text{for } I_i \geq 76 \text{ mm/h} \end{cases} \quad (3)$$

Because the rainfall amount caused by some events has too little energy to disturb soil particles, these events should be neglected. The rainfall erosivity in rainfall events (R_j) should only be estimated from the effective rainfall events. According to Wischmeier and Smith (1978), all effective rainfall events can be defined as follows: (1) events in which the accumulative rainfall amount exceeds 12.7 mm, with no rainfall for 6 h either before or after the event, and (2) events in which the accumulative rainfall amount reaches at least 6.35 mm in 15 min. This study proposed a new index that refers to the rainfall erosivity in a rainfall event calculated by the 10-min rainfall data accumulation converted to the hourly rainfall data (R_{10_60j}), as shown in Equation (4):

$$R_{10\_60j} = E_{60j} \times I_{60j} = \sum_{i=1}^{T_i} \left(e_{60i} P_{ji}\right) \times I_{60j} \quad (4)$$

where:

E_{60j} – the kinetic energy calculated by the 10-min rainfall data accumulation converted to the hourly rainfall data (MJ/ha),

I_{60j} – the maximum 60-min rainfall intensity calculated by the 10-min rainfall data accumulation converted to the hourly rainfall data (mm/h),

https://doi.org/10.17221/25/2020-SWR

e_{60i} – the unitary kinetic energy calculated by the 10-min rainfall data accumulation converted to the hourly rainfall data (MJ/mm·ha),

T_i – the total rainfall duration.

Equation (1) indicates that subscripts *i* and *j* denote the number of rainfall data instances and number of rainfall events, respectively. By adding the R_{10_60j} of all the rainfall events in one year, the annual rainfall erosivity calculated by the 10-min rainfall data accumulation converted to the hourly rainfall data (R_{10_60y}) can be expressed as Equation (5):

$$R_{10\_60y} = \sum_{j=1}^{Y} R_{10\_60j} \quad (5)$$

The relationships between the kinetic energy (E_{10j} and E_{60j}) and the maximum rainfall intensity (I_{30j} and I_{60j}) are both linear (Weiss 1964; Yin et al. 2007a). Thus, the following relationship for the rainfall erosivity in a rainfall event calculated by the 10-min rainfall data accumulation converted to the 30-min rainfall data (R_{10_30j}) can be obtained:

$$\begin{aligned} R_{10\_30j} &= E_{10j} \times I_{30j} \\ &= (\alpha_E E_{60j}) \times \alpha_I I_{60j} \\ &= \alpha_E \alpha_I E_{60j} I_{60j} \end{aligned} \quad (6)$$

where:

α_E – the kinetic energy conversion coefficient,

α_I – the maximum rainfall intensity conversion coefficient.

By adopting the simplified notion $\alpha_{Rj} = \alpha_E \alpha_I$, Equation (6) can be rewritten in the following compact form:

$$R_{10\_30j} = \alpha_{Rj} R_{10\_60j} \quad (7)$$

where:

α_{Rj} – the slope coefficient based on the linear regression through the origin.

Equation (7) was used for the evaluation and calibration by analysing the trends in the 10- and 60-min rainfall data. Evaluating this equation involves statistically determining whether R_{10_30y} during R_{10_30j} is proportional to R_{10_60y} during R_{10_60j}. Thus, α_{Rj} may be used as a conversion coefficient to convert the values of R_{10_60j} to the corresponding values of R_{10_30j}.

Because the variation in the coefficient α_{Rj} results from that in coefficient α_I, the relationship between R_{10_30j} and R_{10_60j} is similar for each station among the fifty-one rainfall stations selected, as illustrated in Figure 2. From Equation (7), R_{10_30y} can be formulated as follows:

$$R_{10\_30y} = \sum_{j=1}^{Y} R_{10\_30j} = \alpha_{Rj} \sum_{j=1}^{Y} R_{10\_60j} = \alpha_{Rj} R_{10\_60y} \quad (8)$$

Assuming that α is constant, the relationship between the annual mean rainfall erosivity calculated by the 10-min rainfall data accumulation converted to the 30-min rainfall data (R_{10_30}) and the annual mean rainfall erosivity calculated by the 10-min rainfall data accumulation converted to the hourly rainfall data (R_{10_60}) can be described as in Equation (9):

$$R_{10\_30} = \frac{1}{n} \sum_{Y=1}^{n} R_{10\_30y} = \alpha_{Rj} \frac{1}{n} \sum_{Y=1}^{n} R_{10\_60y} = \alpha R_{10\_60} \quad (9)$$

where:

n – the cumulative number of years (there were 15 years in this study).

As indicated in the preceding analysis, α is approximately constant and can, thus, be calibrated.

RESULTS AND DISCUSSION

Effective rainfall events. Tables 1 and 2 present the basic geographic and rainfall data of the twenty-six rainfall stations in Kaohsiung City and twenty-five rainfall stations in Pingtung County in this study. According to the criteria, 15 221 effective rainfall events were identified using data from these fifty-one rainfall stations (Tables 1 and 2). The shortest

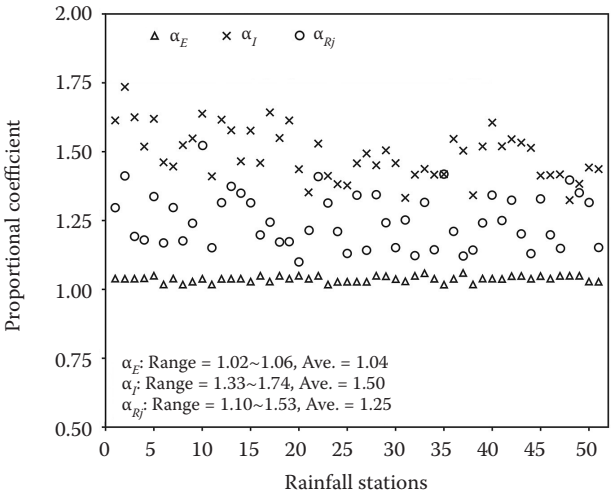

Figure 2. Rainfall energy proportional coefficient α_E, rainfall intensity proportional coefficient α_I, and erosivity proportional coefficient α_{Rj} at the fifty-one rainfall stations

https://doi.org/10.17221/25/2020-SWR

rainfall duration varied from 0.5 to 0.8 h. The longest rainfall duration ranged from 96 to 244 h. The highest accumulated rainfall volume ranged from 522 to 2 970 mm. A maximum 10-min rainfall intensity value of 786 mm/h was observed at the SiaoGuanShan station in Kaohsiung City. The annual rainfall amount varied from 1 358 to 4 070 mm.

Relationship between E_{10j} and E_{60j}. The kinetic energy component of the rainfall erosivity in the Universal Soil Loss Equation (USLE) was computed using Equation (3) for both the 10- and 60-min rainfall data collected from all fifty-one rainfall stations. The significant correlation regression between E_{10j} and E_{60j} with $r^2 = 0.99$ is presented in Figure 3, which can be expressed by Equation (10):

$$E_{10j} = 1.04E_{60j} \quad (10)$$

The difference in the two values of the kinetic energy component was due to the logarithm term in Equation (3). In particular, the hourly data were equal to the sum of six 10-min data values. The variance of E_{10j} and E_{60j} was 0.04. Furthermore, the kinetic energy conversion coefficient α_E varied between 1.02 and 1.06 over the fifty-one rainfall stations and had an average value of 1.04 (Figure 2). The variation in the coefficient ($\alpha_E = 1.04$) in Equation (10) could be obtained by calculating the fixed interval of the 10-min data in E_{10j} and six 10-min data values in E_{60j}, with all the rainfall data derived from the same rainfall event. In addition, the kinetic energy did

Table 1. Rainfall characteristics of the twenty-six rainfall stations in Kaohsiung City

Rainfall station	District	Latitude	Longitude	Effective rainfall events	Shortest rainfall duration (h)	Longest rainfall duration (h)	Longest accumulated rainfall (mm)	Maximum rainfall intensity (mm/h)	Elevation (m)	Annual rainfall (mm)
Zuoying	Zuoying	120°17'N	22°40'E	230	0.5	184	857	101.5	13	1 602
Fengsen	Xiaogang	120°23'N	22°32'E	241	0.5	121	726	84.5	61	1 616
Sanye	Luzhu	120°16'N	22°50'E	366	0.5	122	995	102.5	35	1 635
Gangshan	Qiaotou	120°17'N	22°45'E	259	0.5	125	944	125.5	31	1 617
Gutingkeng	Tianliao	120°24'N	22°53'E	259	0.5	132	1 036	87.5	87	1 421
Mujha	Neimen	120°27'N	22°58'E	224	0.5	137	1 358	109.5	94	2 007
Chishan	Chishan	120°29'N	22°52'E	421	0.5	156	1 789	99.5	63	1 996
Fengsen	Dashe	120°21'N	22°45'E	290	0.5	122	925	126.5	55	1 772
Jiasian	Jiaxian	120°35'N	23°04'E	232	0.5	138	2 094	150.0	60	2 650
XIPU	Dashu	120°26'N	22°43'E	255	0.5	167	1 040	124.5	30	1 903
Fengshan	Fengshan	120°21'N	22°38'E	377	0.5	133	933	105.5	27	1 787
Daliao	Daliao	120°25'N	22°36'E	302	0.5	193	814	85.5	24	1 723
Yuemei	Shanlin	120°32'N	22°58'E	212	0.5	120	1 373	91.0	112	2 271
Meinong	Meinong	120°31'N	22°53'E	307	0.5	117	1 066	121.0	46	2 228
JiaDong		120°33'N	22°50'E	314	0.5	144	1 004	144.5	95	2 257
Jhuzihjiao	Yanchao	120°20'N	22°48'E	310	0.5	123	837	95.0	51	1 799
Jianshan		120°22'N	22°48'E	313	0.5	129	846	109.0	270	1 823
Xinfa	Liugui	120°39'N	23°03'E	256	0.5	139	2 423	148.5	470	3 032
Dajin		120°38'N	22°53'E	427	0.5	120	1 473	156.0	190	2 711
Yuyoushan	Taoyuan	120°42'N	23°00'E	381	0.5	161	2 970	127.0	1 637	4 070
Gaozhong		120°43'N	23°08'E	241	0.5	138	2 338	134.0	760	2 786
Fuxing		120°48'N	23°13'E	380	0.8	117	2 247	122.0	700	2 377
Xiaoguanshan		120°48'N	23°09'E	355	0.5	135	2 541	143.5	1 781	2 995
Sinan		120°48'N	23°04'E	274	0.7	136	2 806	128.5	1 792	3 750
Nantianchi		120°54'N	23°16'E	291	0.8	122	2 740	99.5	2 700	3 661
Paiyun		120°57'N	23°27'E	238	0.8	141	1 655	50.5	3 340	2 642

https://doi.org/10.17221/25/2020-SWR

Table 2. Rainfall characteristics of the twenty-five rainfall stations in Pingtung County

Rainfall station	Township	Latitude	Longitude	Effective rainfall events	Shortest rainfall duration (h)	Longest rainfall duration (h)	Longest accumulated rainfall (mm)	Maximum rainfall intensity (mm/h)	Elevation (m)	Annual rainfall (mm)
Ali	Wutai	120°44'N	22°44'E	263	0.5	141	1 200	108.5	1 040	2 733
Majia	Majia	120°41'N	22°40'E	248	0.7	193	1 939	139.0	740	3 491
Ligang	Ligang	120°29'N	22°47'E	310	0.5	102	1 002	101.5	42	2 016
Pingdong	Pingtung City	120°30'N	22°39'E	292	0.5	167	1 115	115.5	25	2 124
Xinwei	Yanpu	120°32'N	22°45'E	352	0.5	244	1 088	140.5	56	2 222
Linluo	Linluo	120°33'N	22°39'E	234	0.5	167	991	131.5	54	2 230
Nanzhou	Nanzhou	120°30'N	22°29'E	306	0.5	115	867	133.0	20	1 598
Chaojhou	Chaozhou	120°32'N	22°32'E	354	0.5	172	865	154.5	12	1 848
Fangliao	Fangliao	120°35'N	22°21'E	305	0.5	114	707	93.5	69	1 358
Maobitou	Hengchun	120°44'N	21°55'E	342	0.5	99	943	127.5	49	1 419
Checheng	Checheng	120°44'N	22°04'E	320	0.5	105	764	199.5	54	1 610
Laiyi	Wanluan	120°37'N	22°31'E	363	0.5	171	1 355	156.5	74	2 448
Chishan		120°36'N	22°35'E	284	0.5	174	1 789	108.0	48	2 630
Sandimen	Neipu	120°38'N	22°42'E	245	0.5	138	1 299	149.0	59	2 575
Longquan		120°36'N	22°40'E	333	0.5	195	1 045	98.5	61	2 438
Lili	Chunri	120°37'N	22°25'E	228	0.5	168	878	161.5	91	1 944
Chunri		120°37'N	22°22'E	387	0.5	105	708	155.0	86	1 677
Fangshan	Fangshan	120°39'N	22°14'E	197	0.7	118	646	108.0	36	1 627
Shangdewun	Sandimen	120°42'N	22°45'E	395	0.5	140	2 296	173.0	820	3 346
Gusia		120°38'N	22°46'E	395	0.5	201	1 208	116.0	140	2 582
Weiliaoshan		120°41'N	22°49'E	229	0.5	121	2 969	124.5	1 018	3 548
Syuhai	Mudan	120°53'N	22°11'E	227	0.8	120	1 234	100.5	20	2 023
Mudanchihshan		120°50'N	22°09'E	251	0.5	148	566	100.0	504	2 268
Dahanshan		120°44'N	22°06'E	364	0.5	96	522	118.0	260	1 457
Shouka		120°51'N	22°14'E	244	0.5	148	612	81.0	489	2 184

not increase by more than 76 mm/h. The values of E_{10j} and E_{60j} were, thus, substantially equal to each other. Although kinetic energy has been considered the main rainfall erosive factor (Wischmeier & Smith 1958; Hudson 1965; Carter et al. 1974; Sempere Torres 1992), the effect of a high-intensity rainfall on the erosivity was significant in this study area. The high-intensity values were recorded in short periods, particularly in storms with short durations, which indicated that other combinations of the kinetic energy and maximum intensity for shorter periods were more effective erosivity indices for this study area.

Relationship between I_{30j} and I_{60j}. The rainfall intensity component of Equation (1) was computed using the 30- and 60-min rainfall data collected from fifty-one rainfall stations in southern Taiwan. The results for I_{30j} and I_{60j} are shown in Lines 1 and 2 in Figure 4. These lines indicate that the range of variance for I_{30j} was less than $2I_{60j}$, but more than I_{60j}. A difference in the diversity in the rainfall intensity helped identify the relationship among the differing levels of the maximum rainfall intensity. According to all the results, a higher number of rainfall events with a duration less than 30 min resulted in a higher number of I_{30j} values close to $2I_{60j}$. Furthermore, Figure 4 indicates that I_{30j} approached Lines 1 or 2, but the data were located between the two lines if $I_{30j} > 50$ mm/h. The regression analysis revealed the

https://doi.org/10.17221/25/2020-SWR

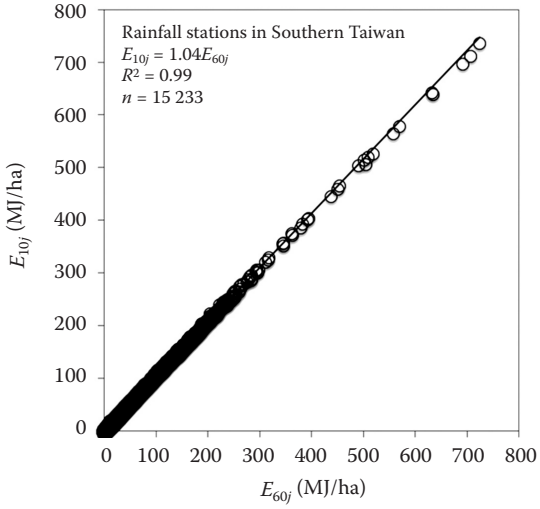

Figure 3. Comparison of the rainfall kinetic energy calculated by the 10-min and hourly rainfall data (E_{10j} and E_{60j})

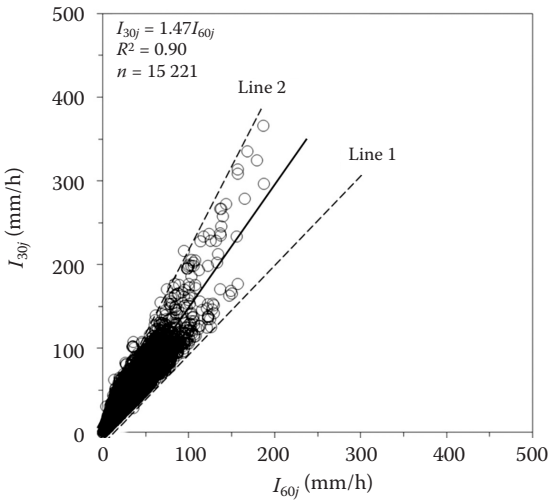

Figure 4. Comparison of the maximum 30-minute rainfall intensity I_{30j} and the maximum hourly rainfall intensity I_{60j}

30- and 60-min rainfall intensity (I_{30j} and I_{60j}) to have the relationship I_{30j} = 1.47I_{60j} (r^2 = 0.90). Here, the maximum rainfall intensity conversion coefficient α_I equalled 1.47. Moreover, Figure 2 indicates that the rainfall intensity conversion coefficient varied more markedly among the fifty-one rainfall stations than did the kinetic intensity conversion coefficient itself. Thus, although the rainfall distribution affected the relationship between I_{30j} and I_{60j}, it was not crucial. Therefore, although the difference between R_{10_30j} and R_{10_60j} was sensitive to the rainfall distribution in a year or a single event, it varied only slightly between the vicinities.

Many studies have assumed that the value of the rainfall erosivity depends entirely on the maximum rainfall intensity and that the conversion factor for the kinetic energy is approximately equal to 1. Yin et al. (2007a) indicated that the dominant role played by I_{30j} on E_j in terms of the error when estimating R_{30j} by using the fixed-interval data was apparent for the 60-min fixed-interval data. The average conversion coefficient was 1.105 for the kinetic energy, and the average conversion coefficient was 1.668 for the maximum rainfall intensity in this research. Our study results had the same variation trend regarding the kinetic energy conversion coefficient and the maximum rainfall intensity conversion coefficient.

Conversion factor for R_{30} and R_{60}. Figure 5 illustrates the relationship between the computed values of R_{10_30j} and R_{10_60j}. The regression analysis revealed that R_{10_30j} and R_{10_60j} with r^2 = 0.97 are related as follows:

$$R_{10\_30j} = 1.30R_{10\_60j} \quad (11)$$

Figure 6 plots R_{10_30} against R_{10_60} with r^2 = 0.95. R_{10_30} and R_{10_60} are expressed as in Equation (12). Here, α equals 1.30.

$$R_{10\_30j} = 1.30R_{10\_60} \quad (12)$$

R_j is underestimated each time the intervals increase from 5, 10, 15, or 30 to 60 min (Williams & Sheridan 1991; Yin et al. 2007a; Panagos et al. 2015). As a compromise, the 30-min temporal resolution data were used, although the most abundant time-step was 60 min. In addition, Yin et al. (2007a) noted that

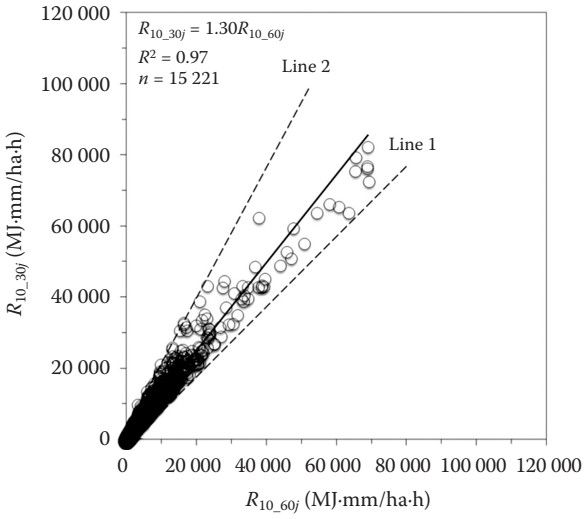

Figure 5. Relationship between R_{10_30j} and R_{10_60j} for each rainfall event

https://doi.org/10.17221/25/2020-SWR

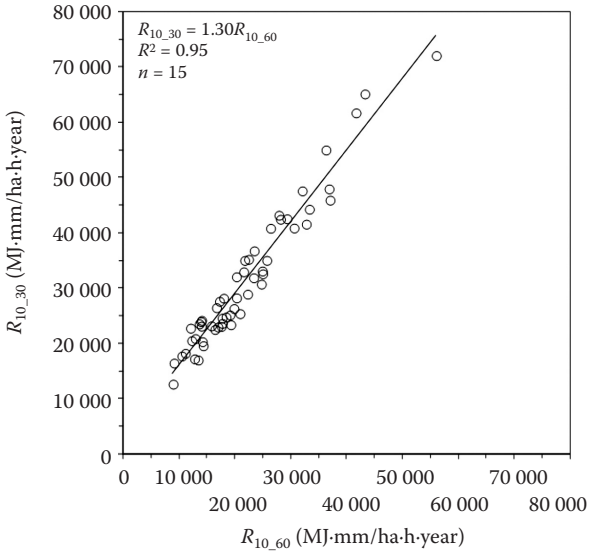

Figure 6. Relationship between R_{10_30} and R_{10_60}

moving toward time intervals less than 30-min to obtain reliable erosivity estimations is unnecessary.

Istok et al. (1986) presented a highly significant linear correlation between R_{15j} and R_{60j} by using the 15- and 60-min data from three sites located at a small watershed in western Oregon. The conversion factors between R_{15j} and R_{60j} varied from 1.193 to 1.378, and statistical differences were evident among the three sites. However, this factor was larger when the breakpoint data were used instead of the 15-min data. Panagos et al. (2015) introduced the regression functions developed to convert R from the different temporal resolutions to the 30-min resolutions. The conversion factors were 1.5597 for R_{60}, 0.8716 for R_{15}, 0.8205 for R_{10}, and 0.7984 for R_5. The conversion factors for the recording time-steps lower than 30 min were less than 1, which explains how the homogenised 30-min-based R dataset slightly overestimated the 'real' rainfall erosivity.

The R originally established by the regression analysis on the annual mean rainfall erosivity and the annual rainfall data recorded from 1957 to 1976 by using 8 rainfall recording rain gauge stations, with only hourly rainfall data (Huang 1979). Unfortunately, these data were not updated almost 30 years ago. This study has established the R_{10_30} based on the 10-min rainfall data from the rainfall stations located in Kaohsiung and the Pingtung area in the tropic region of southern Taiwan. The accuracy of the rainfall data and density of the rainfall stations has been increased during the period of study. The R_{10_30} compared to Huang (1979) showed that most of the R_{10_30} of this study are more reasonably than

Table 3. The significant difference between R_{10_30} based on this study in the tropic region of southern Taiwan (A) and the estimation of Huang (1979) (B)

City/county	Rainfall station	Annual mean rainfall erosivity of this study, R_{10_30} (A)	Annual mean rainfall erosivity of Huang (1979), R (B)	PD = $\frac{(A)-(B)}{(B)} \times 100\%$
		(MJ·mm/ha·h·year)		
Kaohsiung City	Gutingkeng	23 982	13 361	79.5
	Mujha	31 062	18 603	67.0
	Jiasian	43 504	21 028	106.9
	Fengshan	24 581	13 650	80.1
	Meinong	35 282	23 191	52.1
	Nantianchi	41 355	48 008	–13.9
Pingtung County	Ali	38 716	39 890	–2.9
	Ligang	29 096	19 539	48.9
	Pingdong	32 822	19 301	70.1
	Laiyi	47 441	21 854	117.1
	Sandimen	47 515	24 556	93.5
	Longquan	34 055	18 909	80.1
	Gusia	45 495	24 500	85.7
	Dahanshan	19 700	53 259	–63.0
	Shouka	22 595	46 819	–51.7

PD – percent difference

https://doi.org/10.17221/25/2020-SWR

Huang's results, whose range of percent difference is –63.0 ~ 117.1% (Table 3). When using the annual mean rainfall erosivity of Huang (1979) to estimate soil erosion, the R_{10_30} may be underestimated.

CONCLUSION

Calculating the R_{10_30} and R_{10_60} based on the 10- and 60-min rainfall data from fifty-one rainfall stations in southern Taiwan is the best practice, according to this study.

All the results indicated that the kinetic energy values derived using the two sets of data were strongly related because $E_{10j} = 1.04E_{60j}$ with $r^2 = 0.99$. In addition, the maximum rainfall intensity values of the 30- and 60-min intervals were related because $I_{30j} = 1.47I_{60j}$ with $r^2 = 0.90$. The rescaling (conversion factors) of E was nonsignificant, but the rescaling of I was significant when changing the time resolution from the hourly to the 30-min rainfall data.

The R_{10_30j} associated with a rainfall event and the R_{10_60j} associated with a rainfall event can be expected to be $R_{10\_30j} = 1.30R_{10\_60j}$ with $r^2 = 0.97$. Finally, the R_{10_30} and the R_{10_60} can be expressed as $R_{10\_30} = 1.30R_{10\_60}$ with $r^2 = 0.95$. The 60-min rainfall data were successfully used to estimate the rainfall erosivity, where more precise time resolution data were unavailable. A marked improvement in the predictions between the 60-min data and the 30-min data was achieved in this study.

Because typhoons often strike Taiwan between July and October, it is possible for the R_j associated with the heavy rainfall of a typhoon to surpass R, so the conversion factor of the rainfall erosivity will be larger than the conversion factor of the annual rainfall erosivity.

This study proposed a method of estimating the hourly rainfall erosivity on the basis of the 10-min rainfall data that should greatly assist future studies assessing the effects of climate change, which is a major problem in the world.

Compared with the use of conventional rain gauges, applying radar technology, which has gradually matured, allows for the advanced assessment of how a temporal scale, spatial scale, and position affect the annual mean rainfall erosivity (R; Fischer et al. 2018). In the future, the research team will investigate how the temporal and spatial scales change during a typhoon or a heavy rainfall event and how such changes affect the annual mean rainfall erosivity when sufficient radar rain data will become available in Taiwan.

Acknowledgement: We are grateful to Dr. K.-T. Chen, General Research Service Center, National Pingtung University of Science and Technology for his helpful comments and suggested improvements to this paper.

REFERENCES

Angulo-Martínez M., Beguería S. (2009): Estimating rainfall erosivity from daily precipitation records: a comparison among methods using data from the Ebro Basin (NE Spain). Journal of Hydrology, 379: 111–121.

Arnoldus H.M.J. (1977): Methodology used to determine the maximum potential average annual soil loss due to sheet an rill erosion in Morocco. FAO Soils Bulletins, 34: 39–51.

Ateshian J.K.H. (1974): Estimation of rainfall erosion index. Journal of the Irrigation and Drainage Division, 100: 293–307.

Bonilla C.A., Vidal K.L. (2011): Rainfall erosivity in Central Chile. Journal of Hydrology, 410: 128–133.

Carter C.E., Greer J.D., Braud H.J., Floyd J.M. (1974): Raindrop characteristics in south central United States. Transactions of the ASAE, 17: 1033–1037.

Ferro V., Giordano G., Iovino M. (1991): Isoerosivity and erosion risk map for Sicily. Hydrological Sciences Journal, 36: 549–564.

Fischer F.K., Winterrath T., Auerswald K. (2018): Temporal- and spatial-scale and positional effects on rain erosivity derived from point-scale and contiguous rain data. Hydrology and Earth System Sciences, 22: 6505–6518.

Huang C.T. (1979): Studies on the rainfall erosion index in Taiwan. Journal of Chinese Soil and Water Conservation, 10: 127–144. (in Chinese with English abstract)

Hudson N.W. (1965): The influence of Rainfall on the Mechanics of Soil Erosion. [MSc, Thesis.] Cape Town, University of Cape Town.

Istok J.D., McCool D.K., King L.G., Boersma L. (1986): Effect of rainfall measurement interval on EI calculation. Transactions of the ASAE, 29: 730–734.

Lawal O., Thomas G., Babatunde N. (2007): Estimation of potential soil losses on a regional scale: a case of Abomey-Bohicon region. Benin Republic. Agricultural Journal, 2: 1–8.

Laws J.O., Parsons D.A. (1943): The relation of raindrop size to intensity. Transactions of the American Geophysical Union, 26: 452–460.

Lee J.H., Heo J.H. (2011): Evaluation of estimation methods for rainfall erosivity based on annual precipitation in Korea. Journal of Hydrology, 409: 30–48.

Lobo G.P., Bonilla C.A. (2015): Effect of temporal resolution on rainfall erosivity estimates in zones of precipitation caused by frontal systems. Catena, 135: 202–207.

https://doi.org/10.17221/25/2020-SWR

Panagos P., Ballabio C., Borrelli P., Meusburger K., Klikc A., Rousseva S., Tadić M.P., Michaelides S., Hrabalíková M., Olsen P., Aalto J., Lakatos M., Rymszewicz A., Dumitrescu A., Beguería S., Alewell C. (2015): Rainfall erosivity in Europe. Science of the Total Environment, 511: 801–814.

Panagos P., Borrelli P., Spinoni J., Ballabio C., Meusburger K., Beguería S., Klik A., Michaelides S., Petan S., Hrabalíková M., Olsen P., Aalto J., Lakatos M., Rymszewicz A., Dumitrescu A., Perčec Tadić M., Diodato N., Kostalova J., Rousseva S., Banasik K., Alewell C. (2016): Monthly rainfall erosivity: Conversion factors for different time resolutions and regional assessments. Water, 8: 119.

Panagos P., Borrelli P., Meusburger K., Yu B., Klik A., Jae Lim K., Yang J.E., Ni J., Miao C., Chattopadhyay N., Sadeghi S.H., Hazbavi Z., Zabihi M., Larionov G.A., Krasnov S.F., Gorobets A.V., Levi Y., Erpul G., Birkel C., Hoyos N., Naipal V., Oliveira P.T.S., Bonilla C.A., Meddi M., Nel W., Al Dashti H., Boni M., Diodato N., Van Oost K., Nearing M., Ballabio C. (2017): Global rainfall erosivity assessment based on high-temporal resolution rainfall records. Scientific Reports, 7: 4175.

Plangos P., Udmale P. (2017): Impacts of climate change on rainfall erosivity in the Huai Luang watershed, Thailand. Atmosphere, 8: 143.

Renard K.G., Freimund J.R. (1994): Using monthly precipitation data to estimate the R-factor in the revised USLE. Journal of Hydrology, 157: 287–306.

Richardson C.W., Foster G.R., Wright D.A. (1983): Estimation of erosion index from daily rainfall amount. Transactions of the ASAE, 26: 153–156.

Roux J.J.L., Morgenthal T.L., Malherbe J., Pretorius D.J., Sumner P.D. (2008): Water erosion prediction at a national scale for South Africa. Water SA, 34: 305–314.

Sempere Torres D. (1992): Quantification of soil detachment by raindrop impact: Performance of classical formulae of kinetic energy in Mediterranean storms. In: Proc. Oslo Symp. Erosion and Sediment Transport Monitoring Programmes in River Basins, Oslo, August, 1992. IHAS Publication No. 210: 115–124.

Weiss L.L. (1964): Ratio of true to fixed-interval maximum rainfall. Journal of the Hydraulics Division, 90: 77–82.

Williams R.G., Sheridan J.M. (1991): Effect of measurement time and depth resolution on EI calculation. Transactions of the ASAE, 34: 402–405.

Wischmeier W.H. (1959): A Rainfall erosion index for a Universal Soil-Loss Equation. Soil Science Society of America Journal, 23: 322–326.

Wischmeier W.H., Smith D.D. (1958): Rainfall energy and its relationship to soil loss. Transactions of the American Geophysical Union, 39: 285–291.

Wischmeier W.H., Smith D.D. (1978): Predicting Rainfall Erosion Losses – A Guide to Conservation Planning. Agricultural Handbook No. 282, Washington, USDA.

Xin Z., Yu X., Li Q., Lu X.X. (2010): Spatiotemporal variation in rainfall erosivity on the Chinese Loess Plateau during the period 1956–2008. Regional Environmental Change, 11: 149–159.

Yang S.Y., Jan C.D, Huang W.S., Tseng K.H. (2010): Application of hourly data to estimate the rainfall erosivity index. Journal of Chinese Soil and Water Conservation, 41: 189–199. (in Chinese with English abstract)

Yin S., Xie Y., Liu B., Nearing M.A. (2015): Rainfall erosivity estimation based on rainfall data collected over a range of temporal resolutions. Hydrology and Earth System Sciences, 19: 4113–4126.

Yin S., Xie Y., Nearing M.A., Wang C. (2007a): Estimation of rainfall erosivity using 5- to 60-minute fixed-interval rainfall data from China. Catena, 70: 306–312.

Yin S., Xie Y., Wang C.G. (2007b): Calculation of rainfall erosivity by using hourly rainfall data. Geographical Research, 3: 541–547.

Yu B., Rosewell C.J. (1996): A robust estimator of the R-factor for the universal soil loss equation. Transactions of the ASAE, 39: 559–561.

Zhang W.B., Xie Y., Liu B.Y. (2002): Rainfall erosivity estimation using daily rainfall amounts. Scientia Geographica Sinica, 22: 706–711. (in Chinese with English abstract)

Received: February 27, 2020
Accepted: October 10, 2020
Published online: November 16, 2020